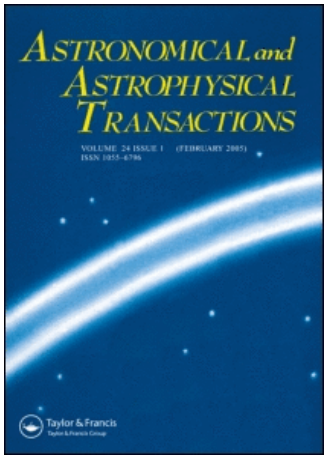

Astronomical & Astrophysical Transactions
The Journal of the Eurasian Astronomical Society
Publication details, including instructions for authors and subscription information:
http://www.informaworld.com/smpp/title~content=t713453505

Algorithms for searching for gamma-gravity correlations

Bonifazi; Pallottino; Gusev; Kochetkova; Postnov; Rudenko; Vinogradov

Online Publication Date: 01 January 2003
To cite this Article: Bonifazi, Pallottino, Gusev, Kochetkova, Postnov, Rudenko and Vinogradov (2003) 'Algorithms for searching for gamma-gravity correlations', Astronomical & Astrophysical Transactions, 22:4, 557 - 578
To link to this article: DOI: 10.1080/1055679031000106565
URL: http://dx.doi.org/10.1080/1055679031000106565

Astronomical and Astrophysical Transactions
Vol. 22, Nos. 4–5, August–October 2003, pp. 557–578

ALGORITHMS FOR SEARCHING FOR GAMMA–GRAVITY CORRELATIONS

P. BONIFAZI[a,c], G. V. PALLOTTINO[a,c], A. V. GUSEV[b,*], A. YU. KOCHETKOVA[b], K. A. POSTNOV[b], V. N. RUDENKO[b] and M. P. VINOGRADOV[b]

[a]Dipartimento di Fisica, Università di Roma 'La Sapienza' Roma, Italy;
[b]Sternberg Astronomical Institute, Lomonosov Moscow State University, Universitetskij Prospekt 13, Moscow 119992, Russia;
[c]Istituto Fisica Spazio Interplanetario, Consigno Nazionale delle Ricerche, Roma, Italy

(Received 11 November 2002)

We report the development of algorithms for searching for possible correlations between the data from gravitational-wave and gamma-ray detectors due to common astrophysical sources. We account for the time delay between the two signals and also use information on the detailed time structure of individual gamma-ray bursts (GRBs). Three possible algorithms of data processing are suggested with different degrees of noise smoothing. The algorithms have been tested using real Burst and Transient Search Experiment (BATSE) GRB data and records of the cryogenic resonant bar detector Explorer. The expected filtering properties of the algorithms are confirmed by the tests. The use of more extended data records is required to detect any correlations or to establish upper limits. A possible generalization for non-Gaussian noises is discussed.

Keywords: Gamma burst; Gravitational wave

1 INTRODUCTION

The modern understanding of the nature of two astrophysical phenomena, namely gravitational wave (GW) bursts and gamma-ray bursts (GRBs), suggests that both phenomena may have common progenitors: superdense relativistic stars at the moment of some catastrophic events in their evolution, such as binary coalescence, stellar core collapse and fragmentation (for a recent GW review, see Grishchuk et al. (2000); for GRB models see Piran (1999) and references therein). There are several more or less elaborate scenarios of such events with associated GW and GRB phenomena, which can be briefly described as follows.

The GRB phenomenon is thought to result from expansion of a hypothetical relativistic photon–lepton fireball with small baryonic load in the surrounding medium (Rees and Meszaros, 1992). The energy of the fireball must be about 10^{51}–10^{54} erg to be consistent with the observed gamma-ray (GR) fluxes of GRBs with measured red shifts (see for example Postnov (2000) and references therein). The fireball itself can be generated by the known astrophysical catastrophic events mentioned above, although quite unexpected 'new physics' are not excluded as well (see the review by Blinnikov (2000)).

* Corresponding author. root@hp.nnov.su

ISSN 1055-6796 print; ISSN 1476-3540 online
DOI: 10.1080/1055679031000106565

A rather definite GW–GRB correlation is expected from relativistic binary coalescence (BC). In this scenario, first a GW burst is generated (e.g. during the binary inspiral stage), and then a GRB appears during the relativistic fireball expansion in the subsequent hydrodynamic stage of merging (Blinnikov et al., 1984; Piran, 1999). Theoretical estimates of the time delay between the GW and GRB have a large uncertainty; according to some estimates (Thorne, 1995), this delay lasts up to 10 s. See also Lipunova and Lipunov (1998) for more estimates and further discussion.

There is increasing observational evidence that at least some long cosmic GRBs, which include more than half of all known GRBs, are associated with star-forming regions in remote galaxies (see Postnov (2000) and references therein), which implies that plausible GRB sources are collapses of very massive stars (for the collapsar models, see Woosley (1993) and Paczynski (1998)). Thp GW–GRB delay in this model can be determined by two characteristic times. The first is the hydrodynamic time of the collapse, which is of the order of $\tau_{\rm hd} \propto (G\rho)^{-1/2}$ for the typical 'precollapse' density of about 10^9–10^{10} g cm^{-3}; this gives the delay estimate as 1 s. Another time scale refers to the neutrino diffusion from the opaque neutrino sphere of a hot protoneutron star which must precede the 'fireball' stage; in this case the delay should be of the order of 10 s (Nadyozhin, 1978).

According to one particular model of this class (MacFadyen and Woosley, 1999), the energy for the fireball stage comes from the accretion of matter on the newborn compact object. Since GRBs are expected to form during the collapse itself, the GW–GRB delay time in this case can in principle be less than the neutronization time (accretion can start on the protoneutron star), that is of the order of several seconds.

Some collapsar models invoke a 'multistage collapse' scenario, when the compact remnant is formed after some intermediate stages. This occurs in a much more complex (and less definite) way. For example, in the model discussed by Imshennik (1992), an initially rapidly rotating stellar core disrupts into two neutron stars forming a close binary system, which coalesces according to the BC scenario. In such models, several relatively compact groups of neutrino bursts, GRBs and GW bursts separated by hours and even longer time intervals can be expected. Clearly, there is not any firm restriction on the time position of the GW burst relative to the GRB in this case. For example, it is possible that first a GW burst can appear during the core collapse and then the second GW chirp signal appears during the binary neutron star coalescence which can initiate a GRB in the end.

A particular case of the multistage scenario is the 'supernova' model (Vietri and Stella, 1999). In this model, first a neutron star with a very strong magnetic field is formed and then it expels the envelope by the magnetorotational mechanism. A GW burst can be produced during this process. Then the neutron star collapses into a final black hole (e.g. as a result of fall-back accretion), which can be accompanied by both GR and GW radiation pulses. It is very difficult to forecast definitely the delay time between these two stages; it might be hours or even years.

All these scenarios assume that the sources are at cosmological distances, They require high-mass stars and a sizeable fraction of the energy converted into GRs to provide a huge intensity of GRBs.

Although the galactic origin of cosmic GRBs is almost ruled out by the present observations (especially for long GRBs), it is worthwhile briefly discussing possible Galactic GW sources which in principle could be potential progenitors for short GRBs. Conventional collapses associated with supernova explosions in the Galaxy and its close environment (30 Mpc) can also produce expanding envelopes encountering the interstellar medium (i.e. usual supernovae) and can form superdense central unstable cores with shock waves

and fragmentation. So in principle they also can be considered as sources of combined GRB–GW radiation. However, for close core collapses it is difficult to obtain the required rate of events (about 1000 GRBs per year), since on average the collapse of a massive star occurs once per 30–60 years per galaxy, and the local density of galaxies is about 0.01 Mpc^{-3}. The same restriction applies to models involving accretion of the relativistic star of $(10^2–10^3)M_\odot$ on the Galactic central black hole with $(10^5–10^6)M_\odot$ (Thorne, 1995) and star-quakes of the pulsars with strong magnetic field (Bisnovatyi-Kogan, 1995; Komberg and Kompaneets, 1997), which also could produce combined GW–GRB signals.

In any case, in both cosmological or Galactic scenarios, the expected amplitude of GW bursts is estimated to be very small, $h \approx 10^{-21}–10^{-23}$, which means that detection (if possible) can be realized only by the accumulation of many individual burst reactions (say 1000 or 10,000 events) on the detector's output. The effectiveness of the accumulation directly depends on a priori knowledge of the time position of the GW bursts with respect to the GR pulses. As we already noted, there is a large uncertainty in just this point. Nevertheless, in the framework of the above scenarios, some algorithms for 'accumulative detection' has been proposed (Modestino et al., 2000), taking into account the signal processing typical for cryogenic bar detectors that are operating at present.

2 SPECIFICS OF THE GRAVITATIONAL WAVE DETECTOR'S OUTPUT

The output signal of a resonant bar detector equipped with a displacement transducer can be described by a two-mode narrow-band process (Astone et al., 1997):

$$x(t) = \sum_{i=1}^{2} r_i(t) \cos[\omega_i t + \vartheta_i(t)] = r(t) \cos[\omega_0 t + \vartheta(t)].$$

The slow variable $r^2(t)$ is proportional to the total energy of the system:

$$r^2(t) = r_1^2(t) + r_2^2(t) + 2r_1(t)r_2(t) \cos[2\Omega t + 2(\vartheta_1(t) - \vartheta_2(t))].$$

$\omega_i = \omega_0 + (-1)^i\Omega$ are the mode eigenfrequencies and ω_0 the central frequency of the detector with $\Omega \ll \omega_0$; $r_i(t)$ and $\vartheta_i(t)$ are the mode amplitudes and phases. The detector output undergoes some optimal processing (Astone et al., 1993). For example, the quadrature components of each mode pass through a Wiener–Kolmogorov filter after lock-in amplifiers (Astone et al., 1997); then they are squared and summed resulting in the variable $\rho_i^2(t)$, which is the mode energy innovation (i.e. the variation in the energy during the filter characteristic time). The total energy innovation is proportional to the sum

$$E(t) = \rho_1^2(t) + \rho_2^2(t).$$

E(t) is the observable variable that we use for the signal detection problem. Alternative variables could be $\rho^2(t) = \min[\rho_1^2(t), \rho_2^2(t)]$ (Bonifazi et al., 1978) or the average value of $\rho_1(t)$ and $\rho_2(t)$ weighted with the corresponding effective mode temperatures (Mauceli et al., 1996).

In our analysis we shall consider first the detection algorithms based on processing just the variable E(t). We also report some results obtained using $\rho^2(t)$.

3 MODEL OF THE SIGNAL AND LIKELIHOOD RATIO

According to the astrophysical prognosis it is reasonable to model the signal s(t) from the GW detector as some non-coherent packet of rare pulses with stochastic amplitudes, random initial phases and unknown arrival times t_i, $i = 1, \ldots, N$. Then, in general,

$$x(t) = \lambda s(t) + n(t), \qquad \lambda = (0, 1).$$

The problem of detecting this signal on a Gaussian noise background n(t) leads to the specific form of the likelihood ratio (see details in the paper by Rudenko et al. (2000)) which is factorized as follows:

$$\Lambda = \prod_{i=1}^{N} \Lambda_i,$$

where Λ_1 is the likelihood ratio of the individual pulse signal and the 'sufficient statistics' $Z = \ln A$ reduce to the form

$$Z = Z(\tau) = \frac{1}{N} \sum_{i=1}^{N} z_i(\tau), \qquad z_i(\tau) = E(\tau_i - \tau + \delta t). \tag{1}$$

In Eq. (1) the following times are introduced: τ_i, times of observed astrophysical events, τ, some unknown time shift between the astrophysical event and possible GW signal; δt, a delay time in the receiver channel. The meaning of the Z variable is clear; it is the selective mean value of the gravitational detector energy innovations corresponding to the observed astrophysical events.

4 STRUCTURE OF 'GAMMA–GRAVITY CORRELATION' ALGORITHMS

Our approach for searching for 'astro–gravity correlations' is based on the idea of examining the data of the gravitational antenna (mostly noise background) in the vicinity of the time marks of astrophysical events observed by other observation channels, that is using other kinds of detector. Then, referring to some specific astrophysical scenario, one could introduce a (common but unknown) time shift with respect to the event time marks, therefore checking the GW detector data before (or later than) the astrophysical events.

Such a programme was realized for example in the case of the 'neutrino–gravity correlation effect' reported at the time of SN1987A (Amaldi et al., 1987; Aglietta et al., 1989; 1991). In that case the neutrino marks were well defined. However, for the GRBs the situation is much more difficult.

The problem is in the large diversity of the time structure and duration of GRBs so that it is very difficult to define a certain 'reference time mark' for those events. The trigger times provided in the BATSE GRB catalogue, as in any other catalogue, have only a very remote relation to the phase of 'real GR production' by the GRB source. Thus the definition of the event time marks requires special care in the development of the gamma–gravity correlation algorithms.

Below we consider several possible approaches to this problem. The general idea of all these attempts is to find in the complex time structure of GRB some specific time mark (let us say 'an effective mark of a gamma pulse' or 'an effective arrival time'), which provides the best representation as the 'reference time mark' of the GRB astrophysical event. By 'best' we mean that such marks should optimize the search for gamma–gravity correlations.

A more general approach consists in taking into account all the time moments of the GRB event structure using proper weights; for example these weights might be proportional to the corresponding fluency bins. Then each sample of the gravitational energy innovation contributing to Eq. (1) is replaced by the integral

$$z_i(\tau) = \int_{-\infty}^{\infty} W_i(\eta) E(\eta - \tau + \delta t)\, d\eta, \tag{2}$$

where $W_i(\eta)$ is the probability density for the arrival time of GRBs; in fact, $W_i(\eta)$ defines a time window in which the integral (2) is not zero. This window corresponds approximately to the duration of the GRB (supposed to be much less then the average interval between events).

Equations (1) and (2) show that to construct an optimal detection algorithm it is desirable to have a priori information about the possible form of the probability density $W_i(\eta)$. One can hope to obtain such information from additional astrophysical data or elsewhere. In this paper we consider the simplest case when the time shift τ between the gravitational and gamma pulses is the same for all observed events (sources of the same type located approximately at the same red shift), that is

$$t_i = \tau_i - \tau, \qquad i = 1, 2, \ldots, N, \tag{3}$$

where the delay time τ is defined by the corresponding astrophysical scenario but in any case it has an upper limit $0 \leqslant \tau \leqslant \Delta$. However, we are aware of other, less exacting (as only based on the GRB trigger times) possibilities, such as those reported by Astone et al. (1999).

We consider in what follows three possible methods for determining the 'effective arrival time' of a GRB using knowledge of its time structure $G_i(t)$. The technique for extracting the G(t) from the observations of the GRB developed by Mitrofanov et al. (1999) is presented in Figure 1 (see some explanation in Section 6) while Figure 2 gives examples of wave shapes for the GRBs which are used in our analysis later.

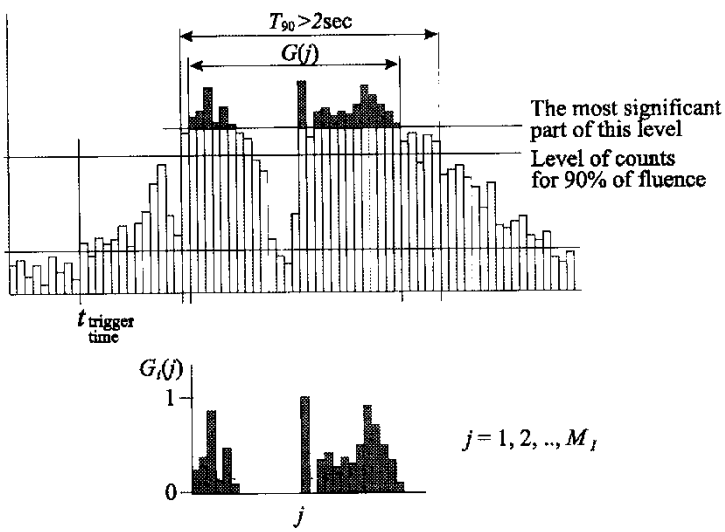

FIGURE 1

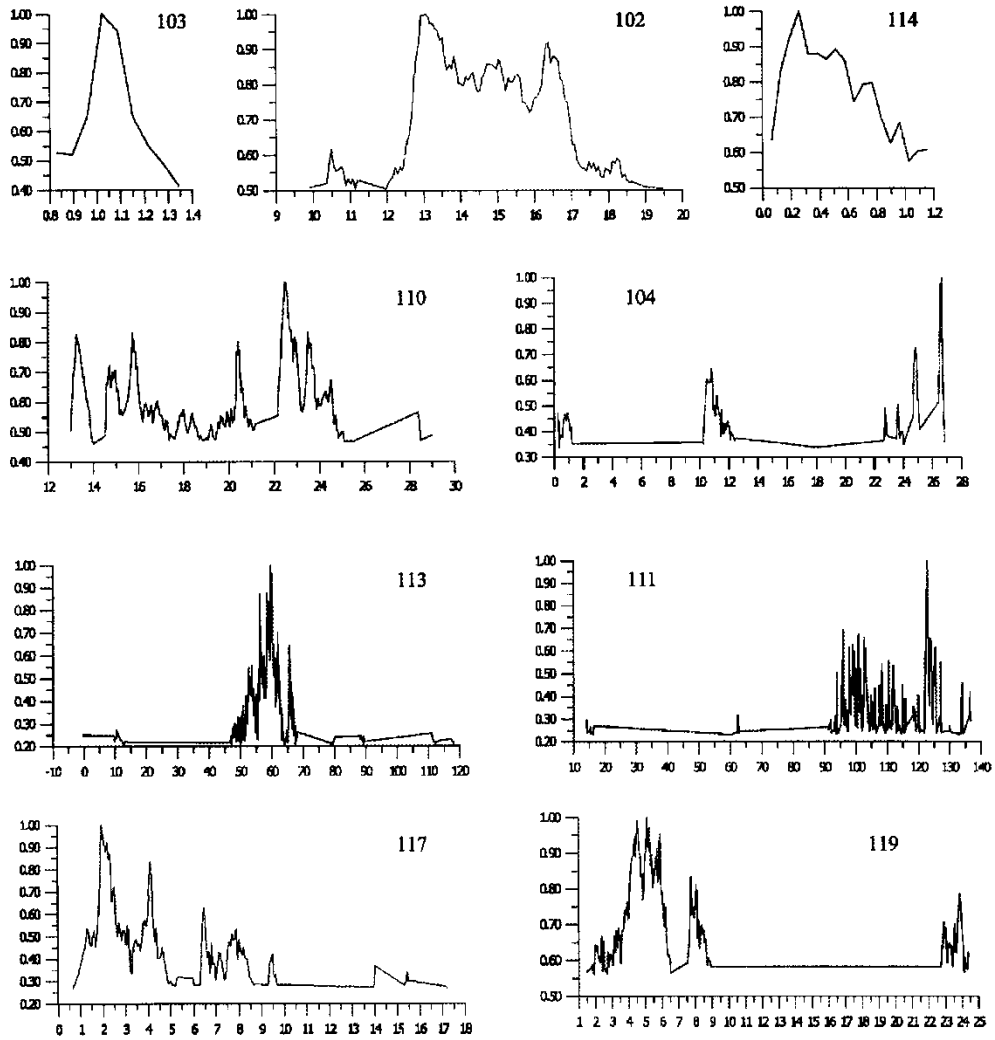

FIGURE 2

4.1 Standard Method of Time Position Evaluation (Standard Method Algorithm)

In this method a conventional definition of the 'mass centre' τ_i^* of the form function $G_i(t)$ according to

$$\tau_i^* = \frac{\int_{-\infty}^{\infty} tG_i^2(t)\,dt}{\int_{-\infty}^{\infty} G_i^2(t)\,dt}. \tag{4}$$

as well as of the effective duration T_i according to

$$T_i = \left(\frac{\int_{-\infty}^{\infty} (t-\tau_i^*)^2 G_i^2(t)\,dt}{\int_{-\infty}^{\infty} G_i^2(t)\,dt}\right)^{1/2} \tag{5}$$

are taken as the average value and the standard deviation of the random variable effective arrival time τ_i. If one chooses a uniform distribution for the probability density $W_i(t_j)$ in the interval $\tau_i^* \pm T_i/2$, then the algorithm (1) and (2) (in the 'partly Bayesian approach') reduces to

$$Z(\tau) \approx \frac{1}{N}\sum_{i=1}^{N} z_i, \qquad z_i(\tau) = \frac{1}{T_i}\int_{\tau_i^*-T_i/2}^{\tau_i^*+T_i/2} E(\eta - \tau + \delta t)\, d\eta. \tag{6}$$

This standard method (SM) algorithm seems adequate for functions $G_i(t)$ exhibiting a single peak, but we consider it somewhat inappropriate for long multipeak GRB events.

4.2 Homogeneous Discrete Algorithm

For multipeak GRBs we propose the following method. Suppose that $\{\tau_{ik}\}$ is the time position of some local k maximum of the i burst $G_i(t)$ whose amplitude exceeds a given threshold G_c, that is, $G_{ik} \geqslant G_c$. Then one can consider the unknown effective arrival time τ_i as a discrete random variable with the following possibilities:

$$\tau_i \to \tau_{i1}, \qquad \text{or } \tau_{i2}, \qquad \text{or } \ldots, \tau_{ik}, \ldots,$$

where $k = 1, \ldots, m_i$, and m_i is the total number of local maxima of the function $G_i(t)$.

In particular, the probability density $W_i(\eta)$ can be represented by the coefficients p_{ik} proportional to the relative amplitudes of the maxima:

$$W_i(\tau_j) = \sum_{i=1}^{m_i} p_{ik}\,\delta(\tau_j - \tau_{ik}),$$

where

$$p_{ik} = \frac{G_{ik}}{\sum_{l=1}^{m_i} G_{il}} \leqslant 1.$$

Then the sufficient statistics, that we call the homogeneous discrete (HD) algorithm, is represented by the formulae

$$Z(\tau) = \frac{1}{N}\sum_{i=1}^{N} z_i(\tau), \qquad z_i(\tau) = \sum_{k=1}^{m_i} p_{ik}\, E(\tau_{ik} - \tau + \delta t). \tag{7}$$

4.3 Discrete Algorithm with Preference

In the previous method the contributions of all the peaks in the GRB structure were regulated only by the relative amplitude of the peaks, using the coefficients p_{ik}. The order of a peak in the GRB structure (its position in time) was not important. However, as noted in the introduction, there are scenarios in which the 'control reference point' for the selection of the GW data is just the beginning of the GR process. To take this fact into account we modify the previous homogeneous algorithm by introducing a preference factor which decreases the role of subsequent peaks.

We implement this requirement by replacing the weight coefficients p_{ik} by other coefficients g_{ik} chosen in such a way that the contribution of the first peak does not change

but the other peaks progressively lose their influence with their order number. A formal description can be written as

$$g_{i1} = p_{i1}, \qquad g_{ik} = p_{ik} \prod_{l=1}^{k-1} (1 - p_{il}), \qquad k = \overline{2, m_i},$$

with the new normalization constant

$$c_i = \left(\sum_{k=1}^{m_i} g_{ik} \right)^{-1}$$

By substituting these modifications into the probability density $W_i(\eta)$ we finally obtain the preference-modified discrete (PD) algorithm

$$Z(\tau) = \frac{1}{N} \sum_{i=1}^{N} z_i, \qquad z_i(\tau) = c_i \sum_{k=1}^{m_i} g_{ik} E(\tau_{ik} - \tau + \delta t). \tag{8}$$

5 DETECTION STRATEGY AND SUFFICIENT STATISTICS

The first approach proposed above assumes that the time shift τ is a fixed but unknown parameter. In this case, the search for the 'gamma–gravity correlation' can be carried out in terms of 'likelihood variable maximization' by a proper (optimal) choice of the time shift parameter. Then the sufficient statistics will be the maximum of $Z(\tau)$ in the admitted shift interval $0 < t < \Delta$.

The detection procedure is based on the conventional Neyman–Pearson strategy, with estimation of false alarm and false dismissal errors as a function of the threshold level Z_α. The delay $\tau = \tau_{opt}$ provided by $\max[Z(\tau)]$ will also be evaluated simultaneously. The hypothesis of gamma–gravity correlation has to be accepted if

$$Z_m = \max_{0 \leqslant \tau \leqslant \Delta} [Z(\tau)] \geqslant Z_\alpha; \tag{9}$$

here Z_α is the threshold level corresponding to the false alarm probability α:

$$F_m(Z_\alpha) = P(Z_m \leqslant Z_\alpha | \lambda = 0) = 1 - \alpha, \tag{10}$$

where $F_m(z)$ represents the integral distribution function of the random variable Z_m in the case of the absence of GW signals ($\lambda = 0$).

Thus the strategy of searching for 'gamma–gravity correlations' is defined completely by Eqs. (6)–(10). The last step required is to determine an explicit form of the distribution function $F_m(Z)$ to derive the threshold level Z_α.

6 ADAPTIVE PROCESSING OF GRAVITATIONAL DATA

In all the above algorithms the sufficient statistics have the same structures; it is the selected mean value of z_i variables which are proportional to the gravitational detector's energy innovations associated with a sequence of N GRBs in the observation interval (the difference

appears only in the weight coefficients of z_i configuration). If $N \gg 1$, the Z statistics tend to a Gaussian distribution independently of the distribution of $E(\tau_i)$.

One can use this property for performing a preliminary calculation of the threshold Z_α in some semiempirical (adaptive) way. The other possibility is to estimate $F_m(z)$ and Z_α in a completely empirical manner by simulating of GR pulse time positions using the gravitational detector's noise background record. Below we consider these approaches separately.

For a given sequence of GRBs, the Z variable represents a stochastic process which is only a function of the shift τ. To study the GW detector noise, one can observe the variations in $Z = Z(\tau)$ taking arbitrary values of the shift in the observation interval (provided that the GRB sequence stays within the borders of the noise record). In the digital data processing, the continuous process $Z(\tau)$, $\tau \subseteq (-\bar{\tau}, \bar{\tau})$ is replaced by its discrete representation

$$\{Z_k = Z(k\ \delta\tau)\}, \qquad k = 0,\ \pm 1,\ \pm 2, \ldots,\ \pm M, \tag{11}$$

where the interval $[-\bar{\tau}, \bar{\tau}]$ is of the order of the observation time, $\delta\tau$ is the sampling time of the shift argument and $M = [[\bar{\tau}/\delta\tau]]$ is the number of shift steps in the observation interval.

The corresponding discrete representation of the 'sufficient statistics' and the detection rule are

$$Z_m = \max_{0 \leqslant k \leqslant L} Z_k \geqslant Z_\alpha, \tag{12}$$

where $L = [[\Delta/\delta\tau]]$ (assuming that $L \ll M$); this means that the sufficient statistics are formed from the process $Z(\tau)$ (or Z_k) by a maximization procedure in the limited interval of admitted time shifts $\tau \leqslant \Delta$ (or $k \leqslant L$)) and the threshold equation will be

$$P\{\max_{0 \leqslant k \leqslant L} Z \leqslant Z_\alpha | \lambda = 0\} \approx 1 - \alpha. \tag{13}$$

The problem of the 'absolute maximum distribution' for a sequence of quasi-Gaussian correlated variables has a solution (Gusev, 1999) so that, for the threshold with confidence level $1-\alpha$, one can use the following formula:

$$Z_\alpha \approx \bar{Z} + \sigma_z \left[2 \ln\left(\frac{aL}{\pi\alpha}\right)\right]^{1/2}, \tag{14}$$

where $\bar{Z} = (2M)^{-1} \sum_{k=-M}^{M} Z_k$ is the empirical mean value of Z, $\sigma_z^2 = (2M-1)^{-1} \sum_{k=-M}^{M} (Z_k - \bar{Z})^2$ is the empirical variance of the stationary quasi-Gaussian process $Z(\tau)$, $a = (1 - R_0^2)^{1/2}$ and $R_0 = \sigma_z^{-2}(2M-1)^{-1} \sum_{k=-M}^{M} (Z_k - \bar{Z})(Z_{k+1} - \bar{Z})$ is the correlation coefficient of neighbouring counts.

Equation (14) allows us to perform completely the procedure of data processing for the search for gamma–gravity correlations up to the final determination of the false alarm error under the assumption that the E(t) variable is Gaussian. However, it is possible to develop a fully empirical procedure for estimating the Z_m distribution in a manner similar to that utilized in the work on the neutrino–gravity correlation effect during the SN1987A. Here the RTM collaboration used a Monte Carlo simulation of neutrino time marks on the observation interval to obtain the required distributions of sufficient statistics (Aglietta et al., 1989; 1991).

In the case of GRBs, as the first approximation, some simpler simulation can be performed (to save the computation time).

Let us divide the total observation interval (the record from the GW detector) into segments of length Δ; the total number of segments is $Q = 2\bar{\tau}/\Delta$ if they touch with each other. Each subinterval contains $k = \Delta/\delta\tau$ data samples and let Z_{mk} be the local absolute maximum of $\tilde{Z}$ inside it. Then the estimate of the integral distribution function for the absolute maximum of $Z(\tau)$ (Eq. (10)) (corresponding to the given realization E(t)) can be represented in the form

$$F_m^*(z) = \frac{1}{Q}\sum_{k=1}^{Q} u(z - Z_{mk}), \tag{15}$$

where u(x) is a 'step function':

$$u(x) = \begin{cases} 1, & x \geqslant 0, \\ 0, & x \leqslant 0. \end{cases}$$

The empirical distribution (18) permits us to evaluate the threshold Z_α in the conventional manner (Eq. (10)) for a fixed level of chance probability α.

More complex and adequate simulation procedures are not forbidden and should be investigated further.

7 PRELIMINARY TESTING OF THE GAMMA–GRAVITY CORRELATION ALGORITHMS FOR THE DATA FROM THE BATSE EXPLORER

The algorithms developed in Section 4 were tested using real data collected by the BATSE observatory (Fishman et al., 1994) and the gravitational wave detector Explorer during the period from February 1, 1994, up to June 1, 1994.

The BATSE data consist of records of GRB profiles in units of integral intensity or 'fluence' (in the energy range $E_\gamma > 25$ keV). Only the bursts with duration parameter $T_{90} > 2$ s (Mitrofanov et al., 1999) were used (their total number was 83). Then according to the method described in the paper by Mitrofanov et al. (1999) the most significant parts of the profiles containing more than half the pulse energy were selected. The final stage of the processing consisted in searching for local maxima for each individual burst profile. These maxima were used for computing the 'mass centre' τ_i^* and the effective duration T_i in the SM algorithm as well as for determining the burst time marks and the corresponding weight coefficients for the HD and PD algorithms.

The Explorer data were given as records of data collected for the two modes $(\rho_1(t), \rho_2(t))$, with sampling time $\Delta t = 0.290\,816$ s, processed using the Wiener–Kolmogorov filter and expressed in kelvins. These modes had roughly equal variances, although some parts of the records had differences of 30–50%. The integral distribution function for both modes had exponential character for relatively small values ($\rho \leqslant \sigma$) with some excess (due to disturbances) at higher energies. The detector energy innovation summed over both modes E(t) was used for further processing with our algorithms (Section 3).

During the considered period of time there are gaps with no data and parts contaminated by large technical noises with anomalous values. For this reason we selected for the analysis only the data with energy below 5 K and standard deviation less than 0.2 K. Finally we obtained 17 parts; some examples are given in Figure 2. These 17 parts were used to calculate the Z statistics for all three types of algorithm discussed in Section 3. The list of GRBs and calculated characteristic times of SM algorithm are given in Table I.

TABLE I GRBs and Calculated Characteristic Times for the SM Algorithm.

BATSE number	Date	Start time	τ_i	T_i
2798	February 6, 1994	0 h 8 min 37.790 s	14.71267	2.01313
2799	February 6, 1994	18 h 25 min 47.672 s	1.06628	0.12664
2812	February 10, 1994	19 h 13 min 16.953 s	15.93025	9.07841
2831	February 17, 1994	23 h 2 min 42.070 s	109.80354	19.93446
2843	February 22, 1994	11 h 50 min 53.078 s	2.29636	2.47170
2855	March 1, 1994	20 h 10 min 37.078 s	19.33162	3.85228
2856	March 2, 1994	5 h 8 min 31.510 s	108.75011	18.56343
2877	March 12, 1994	11 h 28 min 22.680 s	58.36422	8.32440
2880	March 13, 1994	13 h 2 min 22.809 s	0.53577	0.30319
2889	March 19, 1994	23 h 57 min 20.922 s	55.66040	7.84840
2891	March 23, 1994	22 h 4 min 38.430 s	4.40141	2.98549
2897	March 29, 1994	18 h 15 min 37.883 s	8.39619	7.25977
2919	April 10, 1994	15 h 45 min 2.941 s	0.68974	0.80839
2922	April 12, 1994	1 h 40 min 31.000 s	93.45382	18.38526
2925	April 13, 1994	14 h 11 min 24.512 s	5.69802	4.41095
2929	April 14, 1994	16 h 46 min 25.559 s	16.69360	6.02316
2994	May 26, 1994	20 h 20 min 5.789 s	5.38500	2.02936

Gravitational data were taken in the vicinity of GRBs for which the admitted time shift τ did not exceed 100 s.

The Z_{max} statistics were calculated in the empirical manner (see Section 5). About 5×10^6 gravitational data samples were used from the 17 relatively quiet intervals. Using these data we recalculated the Z statistics corresponding to fictitious time positions of GRBs simulated by the Monte Carlo procedure. Then we selected the time shift τ_{opt} that provided a maximum Z. The value $Z_{max}(\tau_{opt})$ gave one point in the Z_{max} distribution.

The final results of our analysis are represented by a number of plots obtained by two independent operators.

8 SUMMARY OF THE DATA PROCESSING

(i) In Figures 3(a), (b) and (c) the Z variable, expressed in kelvins, is plotted as a function of τ for the shift interval ± 30 s using the SM algorithm, the HD algorithm and the PD algorithms respectively. The highest peak is obtained for the shift $\tau \approx 13$ s (this means that the gravitational signals precede the corresponding GRBs). We found that the amplitude of the maximum was reduced by the other algorithms; it equals 0.21 for the SM, 0.18 for the HD method and 0.16 for the PD method. $Z(\tau)$ was calculated also for the wider shift interval of ± 90 s (Fig. 4). For shifts of ± 30 s these plots repeat the previous plots and show new peaks (here smaller than in the ± 30 s range) in the additional regions of τ.

(ii) The empirical distribution functions are reported in Figures 5 and 6 for the shift intervals ± 30 s and ± 90 s respectively, as obtained using the method described in Section 5. By splitting the realization $Z(\tau)$ into Q equal subintervals, one finds a maximum of $Z(\tau)$ in each subinterval $Z_k = \max[Z(\tau)]$, $k = 1, \ldots, Q$. The estimate of the distribution function was obtained using Eq. (18). Figure 3 shows that the probability of the highest peak is quite large (about 0.99 for all methods) for the shift interval ± 30 s. However, it naturally decreases for the longer interval ± 90 s (Fig. 4): $1-\alpha \approx 0.86$ for the peak amplitude 0.2 K using the SM algorithm, $1-\alpha \approx 0.8$ for the peak 0.17 K using the HD algorithm and $1-\alpha \approx 0.76$ for the peak 0.16 K using the PD algorithm.

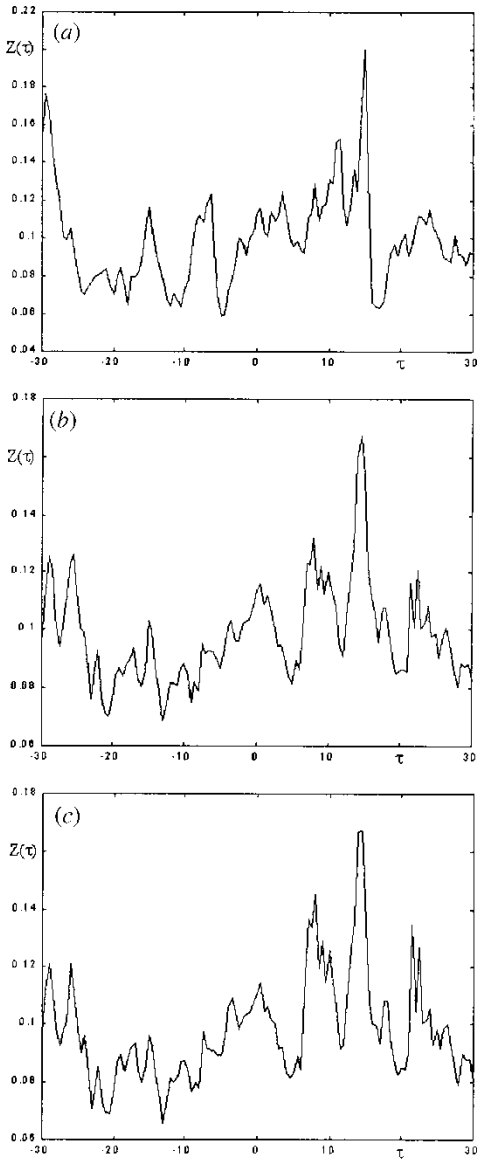

FIGURE 3

(iii) The noise distributions for the two modes are shown in Figure 7, using 94 100 samples for each mode near the 17 bursts mentioned above. They are approximately the same (the solid curve corresponds to ρ_1(t), and the dashed curve to ρ_2(t)).

(iv) When considering the specific GRBs responsible for the effects observed in Figure 1, the following selections were made

(a) Figure 8 represents the Z variable constructed for the group of five bursts mostly contributing to the peak at zero shift (BATSE numbers 2798, 2812, 2855, 2863 and 2891).

(b) Figure 9 corresponds to the group of other five bursts with the Z peak at the shift of 13 s (BATSE numbers 2797, 2815, 2831, 2843 and 2856).

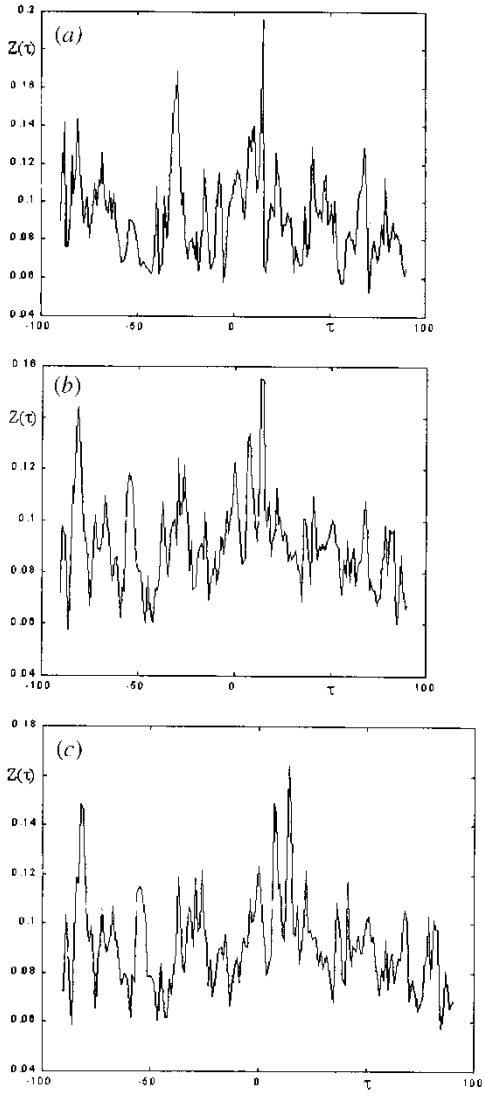

FIGURE 4

(c) Figure 10 corresponds to the remaining seven bursts (BATSE numbers 2799, 2852, 2853, 2877, 2880, 2889 and 2890) with relatively weak amplitudes.

We finally compare the filtering properties of our algorithms denoted by $Z_{m,j}$ the value of the absolute maximum of the stochastic process $Z(\tau)$ for $j = SM, HD, PD$ algorithms and with $F_{m,j}(z)$ its empirical distribution function under the hypothesis that $\lambda = 0$. Then we have $F_{mj}(Z_{m,j}) = 1-\alpha_j$ (see Eq. (13)) where $j = SM, HD, PD$. The relative efficiency of HD and PD algorithms with respect to SM could be defined as γ_{HD} and γ_{PD}:

$$\gamma_{HD} = \frac{\alpha_{HD}}{\alpha_{SM}}, \qquad \gamma_{PD} = \frac{\alpha_{PD}}{\alpha_{SM}}.$$

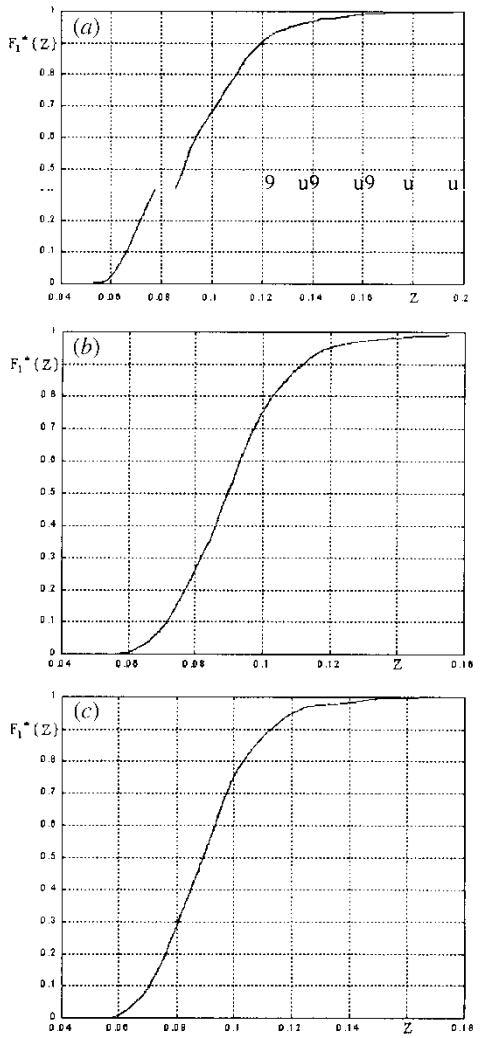

FIGURE 5

These coefficients provide a better representation of the quality of the algorithms HD and PD than the simplest estimation based on the signal-to-noise ratio $q = Z_{mj}/\sigma_j$, j = SM, HD, PD, where σ_j^2 are the variances of the random processes $Z_j(\tau)$.

8.1 Using the Minimum for the Two Modes

We mentioned in Section 2 that the alternative quantity $\rho^2 = \min(\rho_1^2, \rho_2^2)$ could be used as the observed variable. This choice is based on the fact that a short burst of gravitational radiation should excite both modes by the same amount, while a noise pulse may affect the two modes differently. As a consequence, the variable $\rho^2(t)$ provides a better rejection for some disturbances.

We used the quantity ρ^2 to test our algorithms. The corresponding Z variables vs. the time shift τ are given in Figures 11(a), (b) and (c) for the SM, the HD and the PD algorithms respectively. These plots are different from those of Figure 3. In particular there is a

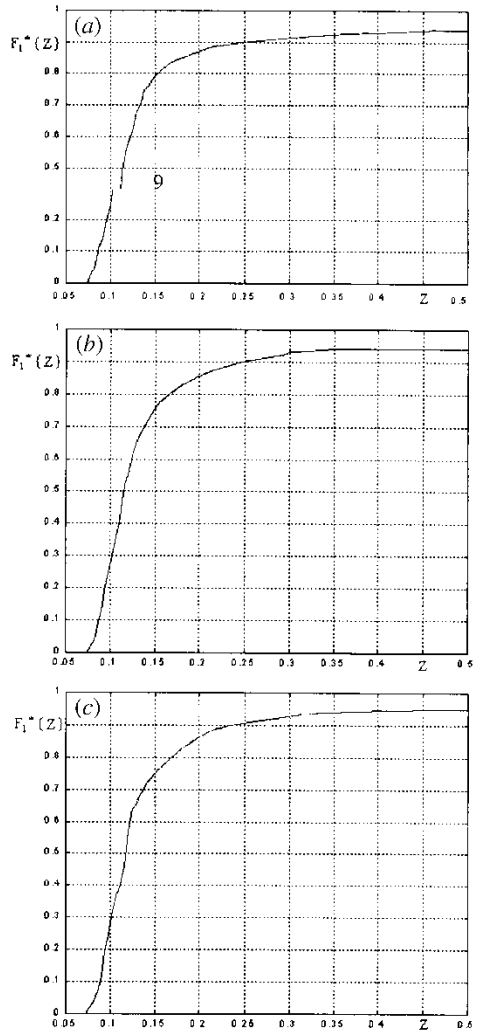

FIGURE 6

maximum for the negative time shift -5 s (i.e. with gamma pulses arriving before the GW detector signals, which contradicts the astrophysical expectations). As before, the smoothing of the noise grows from the SM algorithm to the PD algorithm.

In the present case, the empirical confidence level for Z_m (0.9 for SM, 0.8 for HD and 0.7 for PD) remains similar to that obtained previously, but the limited volume of available data in this test does not allow us to give a preference for any of the algorithms.

9 DEVELOPMENT OF ALGORITHMS FOR A NON-GAUSSIAN BACKGROUND

If the GW detector noise n(t) (Section 2) does not follow a Gaussian distribution, then the variable $Z = \ln \Lambda$ (Eq. (1)) does not correspond any longer to the optimal approach. It has to be replaced by another variable. Below we discuss how one could proceed in this case.

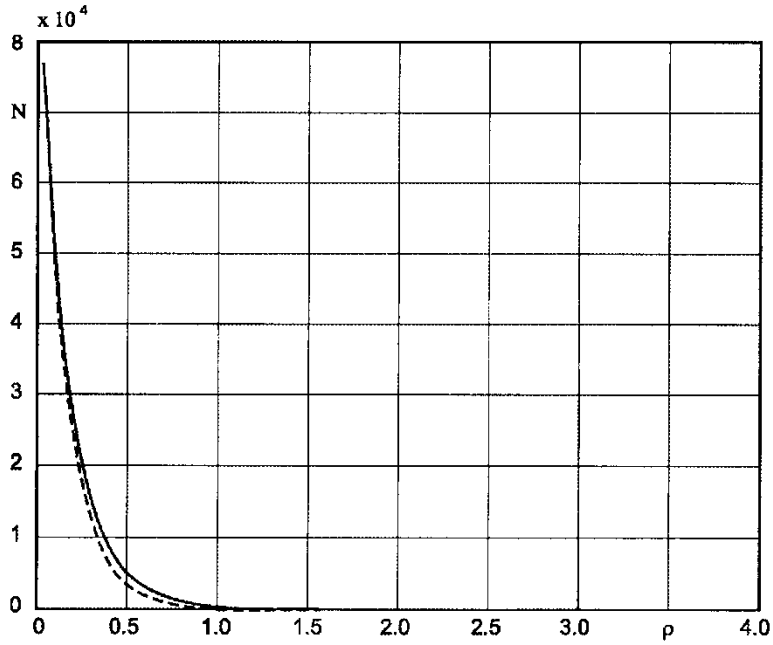

FIGURE 7

Let the response function of a bar detector written in the narrow-band form be (see Section 2)

$$g(t) = g_0(t)\ \cos[\omega_0 t + \psi(t)],$$

where $\omega_0 = (\omega_1 + \omega_2)/2$ is the central frequency of the antenna bandwidth (in the paper by Astone et al. (1997), g(t) was presented as a sum of mode oscillators; it is easy to convert it into the form (16).) Then the packet of signal pulses at the detector's output is

$$s(t) = \sum_k s_k(t), \qquad s_k(t) = a_k g_0(t - t_k) \cos\left[\omega_0(t - t_k) + \psi(t - t_k) + \varphi_k\right].$$

The important point here is that the values (a_k, t_k, φ_k) are unknown stochastic parameters. If no a priori information concerning these values is available, one should use the Bayesian approach, that is the likelihood ratio $\bar{\Lambda}$ averaged over these parameters.

At the output of the fast matched filter $(x(t) \to y(t))$ (Astone et al., 1997) the observable realization remains a narrow-band process:

$$y(t) = s_y(t) + n_y(t) = y_c(t) \cos(\omega_0 t) - y_s(t) \sin(\omega_0 t).$$

By performing the demodulation using a lock-in amplifier with central frequency ω_0, one can obtain the slow quadrature signals $y_c(t)$ and $y_s(t)$ for further processing, containing the noises $n_c(t)$ and $n_s(t)$ and signal components with amplitudes $A_k = a_k \sigma_y^2$, where σ_y^2 is the variance of stationary random process $n_y(t)$.

It is known that, for stationary narrow band processes, a two-dimensional distribution function $W_2(n_c, n_s)$ can be reduced to a one-dimensional distribution of the squared envelope $e(t) = n_c^2(t) + n_s^2(t)$:

$$W_2(n_c, n_s) = \frac{1}{\pi} W(n_c^2 + n^2),$$

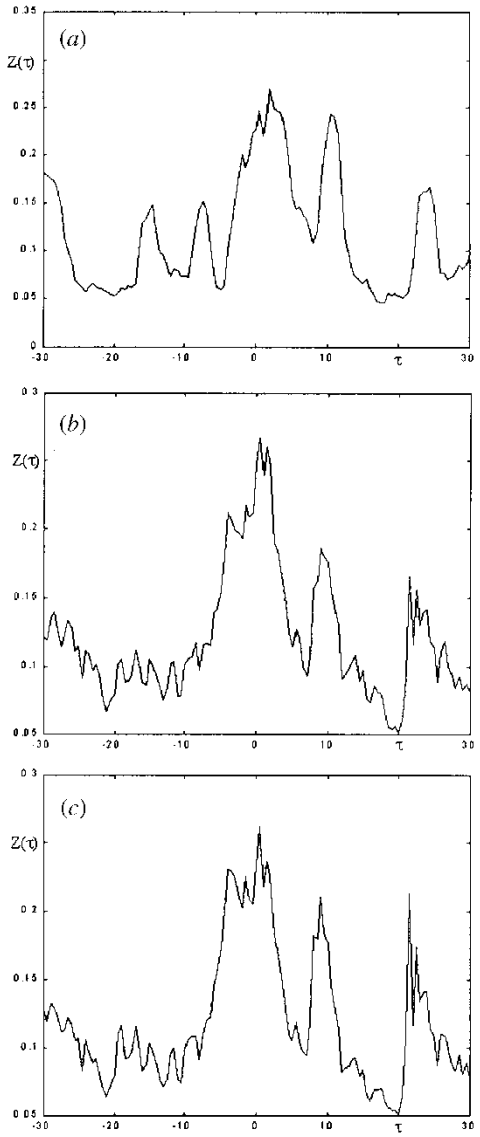

FIGURE 8

where W(e) is the probability density of the envelope $e(t) = n_c^2(t) + n_s^2(t)$. This is because the phase is uniformly distributed in the interval $(0, 2\pi)$ and does not depend on the envelope evolution e(t). Thus all useful information is contained in the envelope's variations. Using the envelope, one can obtain the likelihood ratio in a conventional way. It is factorized on factors $\bar{\Lambda}_k$ of the individual signal pulses. Then it should be averaged over the stochastic parameters A_k and φ_k:

$$\bar{\Lambda} = \prod_{k=1}^{N} \bar{\Lambda}_k, \qquad \bar{\Lambda}_k = \left\langle \frac{W((y_{ck} - A_k \cos\varphi_k)^2 + (y_{sk} - A_k \sin\varphi_k)^2)}{W(y_{ck}^2 + y_{sk}^2)} \right\rangle. \tag{17}$$

The notation $\langle \cdots \rangle_{A_k,\, \varphi_k}$ means statistical averaging, $y_{ck} = y_c(t_k + \Delta t)$ and $y_{sk} = y_s(t_k + \Delta t)$.

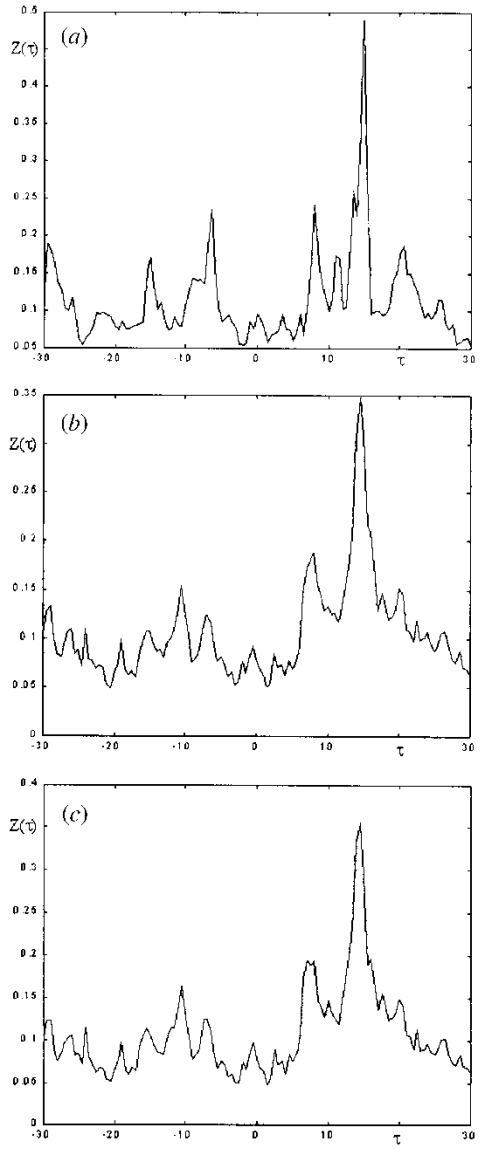

FIGURE 9

For weak signals $A_k \ll \sigma_y$ the likelihood ratio can be expanded in series on the signal amplitude (Rudenko and Gusev, 2000). Then Eq. (17) results in the following approximation:

$$\bar{\Lambda}_k \approx 1 + \frac{\overline{A^2}}{4} f(E_k), \qquad E_k = y_{ck}^2 + y_{sk}^2, \qquad f(E) = \frac{1}{W(E)} \frac{d}{dE}\left(E \frac{dW(E)}{dE}\right), \qquad (18)$$

where $\overline{A^2} = \langle A_k^2 \rangle$ is the mean intensity of the signal pulse.

Equation (18) assumes that the t_k values are defined by observations obtained from other channels. As we have seen in the case of GRBs, there is a large uncertainty in the t_k estimate

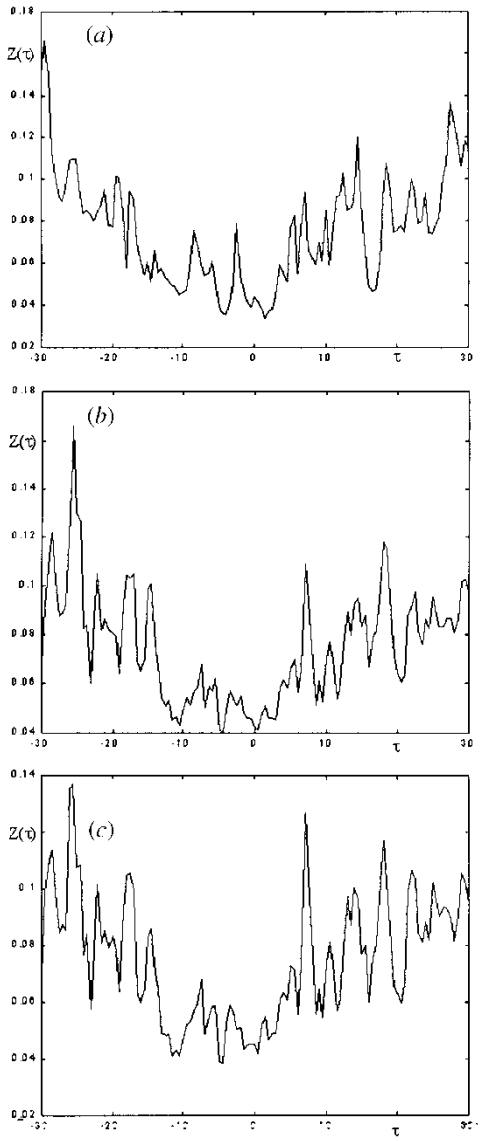

FIGURE 10

due to the very complex structure of GRBs. For this reason, the algorithm (18) should be averaged also over the t_k distribution:

$$\bar{\Lambda}_k \approx 1 + \frac{\overline{A^2}}{4} \langle f\,[E(t_k + \Delta t)] \rangle_{t_k}. \tag{19}$$

Finally, sufficient statistics for searching for the gamma–gravity correlation against a non-Gaussian background can be represented as

$$Z = \text{constant} \sum_k \int_{t_k} f\,[E(\eta + \Delta t)] W_k(\eta)\, d\eta. \tag{20}$$

Here $W_k(\eta)$ is the probability density of the arrival times t_k as in Eq. (2).

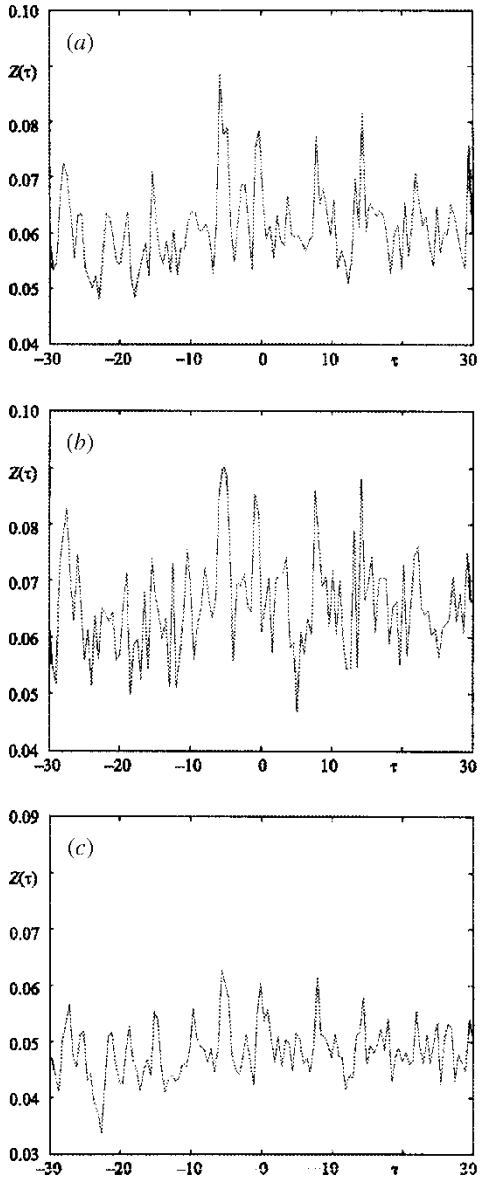

FIGURE 11

In a real experiment the density probability $W_e(e)$ mostly is unknown. Then one could use its parametric approximation. For this purpose a family of Pearson's curves is good (Gusev et al., 1998) as well as poly-Gaussian distributions.

Equation (20) represents a generalization of the gamma–gravity correlation algorithms for non-Gaussian background. In the particular case of Gaussian noise,

$$W_e(e) = (2\sigma^2)^{-1} \exp\left(-\frac{e}{2\sigma^2}\right),$$

the nonlinear algorithm (20) reduces to the previous form similar to Eq. (1): $f(E) = E/2\sigma^2 - 1 \propto E$.

10 CONCLUSIONS

Our test processing of the BATSE Explorer data allows us to come to the following conclusions.

(i) During our tests, several peaks were found above the detection threshold with relatively high confidence level (0.7–0.9) (see Section 7). We believe that this is the result of the non-stationary non-Gaussian excess noise which shows up in the high-energy tail of the gravitational detector data distribution. The empirical distribution function of the absolute maxima (15) obtained by the averaging over shift time subintervals assumes that the detector noise is locally stationary. In reality, the detector's background is contaminated by large non-thermal pulses (excess noise). However, these pulses are rare enough to produce a small influence on the empirical distribution function (due to the time-averaging procedure). Thus such pulses could be detected as some 'false signals' above the threshold corresponding to the 'stationary statistics'.

(ii) Having in mind this conclusion (see i, above), when comparing the tested algorithms, one reasonably gives preference to those which are less sensitive to excess non-stationary noises (i.e. have a decreased property of recording these noises as 'false signals'). The quantitative characteristic of such ability is just the relative efficiency parameter γ introduced in Section 7. This parameter increases from the SM to the PD method; in particular for the shift interval the relative efficiencies are $\gamma_{\mathrm{PD}} \approx 1.71$ and $\gamma_{\mathrm{HD}} \approx 1.42$.

(iii) The confidence limit for real signals decreases in general when we increase the admitted shift interval. This interval can be reduced only with reference to accepted astrophysical source models.

(iv) The tested sample taken to illustrate the data processing appeared to be too short; it contained only 17 GRBs, too small to observe any accumulation effect needed for the detection of weak signals. The recommendation of using longer records (with a duration of 1 year or more) is the obvious conclusion for further studies.

As a final remark we would like to emphasize that the possibility of accumulation of GW pulses strongly depends on a priori astrophysical knowledge of the source nature and so any algorithms of data processing will be 'model dependent'. In particular we used above the simplest model of 'identical GW–gamma radiators' isotropically distributed at distances with equal red shifts; in this case, one can take the same 'gravity–gamma' delay time for all events. More realistic models have to take into account the dependence of the delay time on cosmological distance z, which could be considered as a stochastic parameter with a suitable distribution.

Acknowledgements

The authors express their sincere gratitude to Professor Igor Mitrofanov and members of his group at the Space Research Institute, Russian Academy of Sciences, for providing special profiles of GRBs recorded by the BATSE experiment and very useful discussions. We would also like to thank the Roma Observatory Gravitational (ROG) Rome group and especially Pia Astone for providing the Explorer data. This work was partially supported by the Russian Foundation for Basic Research (Project 00-02-17884), by Istituto Nazionale di Fisica Nucleare and by Ministeo dell'Università e della Ricerca Scientifica e Tecnologica (Project entitled 'Data analysis of gravitational detector' COFIN-2000).

References

Aglietta, M., et al. (1989). Nuovo Cim. C, 12, 75.
Aglietta, M., et al. (1991). Nuovo Cim. C, 14, 171.
Amaldi, E., et al. (1987). Europhys. Lett., 3, 1325.
Astone, P., et al. (1993). Phys. Rev. D, 47, 362.
Astone, P., et al. (1994). Nuovo Cim. C, 17, 713.
Astone, P., et al. (1997). Nuovo Cim. C, 20, 9.
Astone, P., et al. (1999). Astron. Astrophys., Suppl. Ser., 138, 603.
Bisnovatyi-Kogan, G. S. (1995). Astrophys. J., Suppl. Ser., 97, 185.
Blinnikov, S. I. (2000). Surveys High Energy Phys., 15, 37.
Blinnikov, S. I., et al. (1984). Astron. Zh. Pis'ma, 10, 177.
Bonifazi, P., et al. (1978). Nuovo Cim. C, 1, 465.
Grishchuk, L. P., Lipunov, V. M. and Postnov, K. A. (2001). Usp. Fiz. Nauk Physics - Uspehi, 44, 1.
Gusev, A. V., et al. (1998). Proceedings of the 2nd E. Amaldi Conference in Gravitational Waves. World Scientific, Singapore, p. 512.
Gusev, A. V. (1999). Vest. Mosk. Univ., Ser. III, No. 5, 15.
Fishman, G. J., et al. (1994). Astrophys. J., Suppl. Ser., 92, 229.
Imshennik, V. S. (1992). Sov. Astron. Lett., 18, 194.
Komberg, B. V. and Kompaneets, D. A. (1997). Astron. Rep., 4, 611.
Lipunova, G. V. and Lipunov, V. M. (1998). Astron. Astrophys., 329, L29.
MacFadyen, A. and Woosley, S. (1999). Astrophys. J., 524, 262.
Mauceli, G., et al. (1996). Phys. Rev. D, 54, 1264.
Mitrofanov, I. G., et al. (1999). Astrophys. J., 522, 39 805.
Modestino, P., et al. (2000). Astron. Astrophys., 364, 419.
Nadyozhin, D. K. (1978). Astrophys. J., Suppl. Ser., 53, 131.
Paczynski, B. (1998). Astrophys. J., 499, L45.
Piran, T. (1999). Phys. Rep., 314, 575.
Postnov, K. A. (2000). In Proc. I Workshop "Hot Points in Astrophysics," Dubna, Russia, 22–26 August 2000, JINR, 2000, p. 141.
Rees, M. J. and Meszaros, P. (1992). Mon. Not. R. Astron. Soc., 258, 41P.
Rudenko, V. N., et al. (2000). Soviet Phys. JETP, 91, 845.
Rudenko, V. N. and Gusev, A. V. (2000). Int. J. Mod. Phys. D, 9, 353.
Thorne, K. S. (1995). Particles, Nuclear Astrophysics, Cosmology in the Next Millenium. World Scientific, Singapore, p. 160.
Vietri, M. and Stella, L. (1999). Astrophysical J., 527, L43.
Woosley, (1993). Astrophys. J., 405, 273.